Inorganic Chemistry

Article

pubs.acs.org/IC

Revisiting the Spectroscopy of the Bi^{3+} Ion in Oxide Compounds

Philippe Boutinaud*

Clermont Université, ENSCCF, BP 10448, F-63000 Clermont-Ferrand, France

CNRS, UMR 6296, ICCF, F-63173 Aubière, France

ABSTRACT: A model is introduced to predict the energy of metal-to-metal charge-transfer transitions in oxide compounds containing Bi^{3+} ions and d^0 or d^{10} metals (M^{n+}). The model takes into account the structural characteristics of the host lattices, the anion relaxation resulting from Bi^{3+} doping, and the electronegativities and coordination numbers of the Bi^{3+} and M^{n+} ions in the compounds. It is shown, through a critical review of the archival literature, that this model provides new insights on the assignment of the luminescence spectra and the related interpretation of the spectroscopic behaviors.

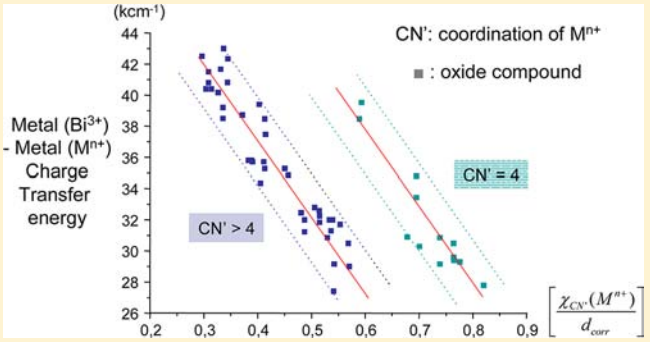

1. INTRODUCTION

Understanding the luminescence behavior of Bi^{3+} ions in solids has been the subject of extensive investigations for more than half a century.[1] Despite all these efforts, the bismuth spectroscopy still presents unclear aspects, with regard to the assignment of the luminescence signals and the related absorption and relaxation processes.[2] It is important to try to clarify this complex situation for the optimal design of phosphors incorporating bismuth as an activator or a sensitizer. A new model is introduced for this purpose in this paper.

We know that (i) the ground state ($^1S_0$) of the isolated Bi^{3+} ion has a $6s^2$ configuration and (ii) electronic transitions to a $6s^16p^1$ configuration raise the excited states $^3P_{0,1,2}$, $^1P_1$, to and from which absorption and emission is achieved. Transitions from $^1S_0$ to $^3P_1$, $^3P_2$, and $^1P_1$ are usually denoted as A, B, and C, respectively. The spin-allowed C transition is usually located far in the ultraviolet (UV) region and will not be considered here. The B transition is spin-forbidden, and its intensity is not expected to be very high. For these reasons, only the A transition will be considered in the present paper. This transition is expected to have reasonable oscillator strength through the spin−orbit mixing that takes place between $^3P_1$ and $^1P_1$. The Bi^{3+} emission is known to cover a very broad spectral range, extending from the UV to the red. The associated Stokes shifts also vary in large proportions. These behaviors are generally taken into account by considering the influence of the nearby chemical environment (coordination number, site symmetry, covalency, host stiffness, etc.)[3] or by invoking an off-center positioning of the Bi^{3+} ion.[4] It is interesting to mention here the original approach of Réal et al., based on an ab initio embedded cluster method that nicely confirms the spectral assignments and spectroscopic behaviors in $Y_2O_3:Bi^{3+}$.[5−7] It is well-known that both $^3P_0$ and $^3P_1$ are emitting states in the isolated Bi^{3+} ion. The transition probability from $^3P_0$ is small and this metastable state acts an an electron trap. The radiative process is interpreted in the frame of a three-level scheme ($^1S_0$, $^3P_1$, $^3P_0$) and is temperature-dependent.[8−11] The energy gap separating these two emitting levels (also referred to as the trap depth) is known to vary with the value of the Stokes shift: the smaller the trap depth, the larger the Stokes shift.[8,12] The interpretation of this effect is still not completely fixed: some authors relate the small trap depths to an excitonic behavior,[13] while others ascribe it to an effect of the coordination number.[12] This question will be reconsidered in light of the new model.

In addition to the $6s^2 \rightarrow 6s^16p^1$ interconfigurational transitions, other Bi-related luminescence signals, of different origin, are also frequently observed. They are sometimes ascribed to Bi clusters or referred to as D-level signals with charge transfer (CT) character. The D-level state is also perceived as a trapped exciton (TE) state (i.e., a bound electron−hole pair with the hole localized on Bi^{3+} and the electron delocalized on the nearest cationic neighbors) or described as a metal-to-metal charge-transfer (MMCT) state.[14] The state is formed by the interaction between the Bi^{3+} levels and the electronic levels of host metal cations (M^{n+}) having d^0 or d^{10} configuration. D-level absorption is then depicted as a transition from the Bi^{3+} ground state to the host conduction band states. Depending on the electronic configuration of M^{n+}, the transition is expressed as $Bi^{3+}(6s^2)/M^{n+}(d^0) \rightarrow Bi^{4+}(6s^1)/M^{(n-1)+}(d^1)$ or $Bi^{3+}(6s^2)/M^{n+}(d^{10}) \rightarrow Bi^{4+}(6s^1)/M^{(n-1)+}(s^1)$. The assignment of these extra signals is still the subject of controversy.[2,15]

Recently, a preliminary empirical model has been developed in order to predict the energy of MMCT states in d^0 transition-metal oxides doped with Bi^{3+} (i.e., titanates, vanadates, niobates, etc.).[16] This energy represents the gap separating the $^1S_0$

Received: February 13, 2013
Published: May 1, 2013

   dx.doi.org/10.1021/ic400382k | Inorg. Chem. 2013, 52, 6028−6038

ground state of Bi^{3+} to the bottom of the conduction band. This raises three possible situations, which are reproduced in Figure 1:

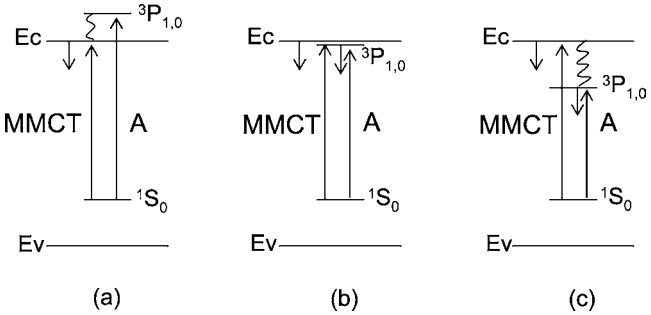

Figure 1. Different configurations of the energy levels leading to luminescence in Bi^{3+}-doped solids.

(a) *The MMCT energy is smaller than the A transition*. In this case, the MMCT state is excited directly and is emitting.[16] The A transition is not excluded. It can be followed by the autoionization of Bi^{3+}, depending on the coupling strength between $^3P_{1,0}$ and the conduction band states. In the case of photoionization, the absorbed energy can be lost nonradiatively or transferred to the MMCT state, with subsequent emission from this latter state.

(b) *The A and MMCT transitions have approximately the same energies*. This means that the $^3P_{1,0}$ states are located close to the bottom of the conduction band. In this case, both MMCT and $^3P_{1,0}$ states should emit, with different relative intensities, depending on the temperature.

(c) *The MMCT energy is larger than the A transition*. Then, emission from the $^3P_{1,0}$ states follows a direct $^1S_0 \rightarrow {}^3P_1$ transition. Excitation of the MMCT state is still possible and can be followed either by MMCT emission or by $^3P_{1,0} \rightarrow {}^1S_0$ emission after transfer of the absorbed energy.

It was shown in ref 16 that the MMCT energy obeys the following empirical equation:

$$\mathrm{MMCT}(\mathrm{Bi}^{3+}, \mathrm{cm}^{-1}) = 46\,000 - 27\,000\frac{\chi_{\mathrm{opt}}(\mathrm{M}^{n+})}{d(\mathrm{Bi}^{3+}\text{–}\mathrm{M}^{n+})} \quad (1)$$

In this equation, $\chi_{\mathrm{opt}}(M^{n+})$ is the optical electronegativity of the d^0 metal cations. The values were extracted from the pioneer work of C. K. Jørgensen.[17] It is useful to note that the $\chi_{\mathrm{opt}}(M^{n+})$ values reported in this work are given for 6-fold-coordinated transition metals in hexahalides. They are only indicative for oxides and do not take into consideration coordination numbers different from 6. The term $d(Bi^{3+}–M^{n+})$ represents the shortest $Bi^{3+}–M^{n+}$ interatomic distances in the host lattices. They were obtained from the Inorganic Crystal Structure Database[18] and were taken between the cation site available for Bi^{3+} and the M^{n+} site. The effect of anion relaxation that occurs after the incorporation of Bi^{3+} in the host lattices was not considered in eq 1.

The present paper follows two objectives:

- Improve the above MMCT model by extending it to d^{10} metals and taking into account the coordination of the M^{n+} ions in the compounds and the anion relaxation that results from Bi^{3+} doping.
- Introduce a user-friendly tool that could facilitate the assignment of the luminescence spectra of Bi^{3+}-doped oxide compounds and make interpretation of the spectroscopic behaviors easier. The luminescence of the Bi^{3+} ion in a selection of oxide compounds is revisited in this paper, in light of this new MMCT model.

2. METHODOLOGY

The starting point of this investigation is the new set of electronegativity (EN) scale published by Li and Xue for elements in different valence states and coordinations.[19] The EN values extracted from this work will be noted as $\chi_{\mathrm{CN}'}(M^{n+})$, where CN′ is the coordination number of M^{n+} cations in the host lattices. In another report, the same authors have shown that these EN values could be relevant for evaluating the charge-transfer energies in CaF_2 and YPO_4 doped with trivalent lanthanides.[20] In a second step, several host lattices activated with Bi^{3+} were selected from the archival literature. For all, the structural properties were collected (from the Inorganic Crystal Structure Database (ICSD)) and the shortest distances between the M^{n+} site(s) and the cation site(s) available for Bi^{3+} (d_{host}) were compiled. These values were corrected to account for the effect of anion relaxation subsequent to Bi^{3+} doping, following a procedure described in ref 21. The corrected distances take the form

$$d_{\mathrm{corr}} = d_{\mathrm{host}} + \frac{1}{2}[r(\mathrm{Bi}^{3+}) - r(\mathrm{host})] \quad (2)$$

where $r(Bi^{3+})$ is the ionic radius of the Bi^{3+} ion and r(host) is the ionic radius of the host cation that is substituted to Bi^{3+}. These radii were taken from the work of Shannon.[22] Referring to this work, the crystal radii were privileged as they correspond more closely to the physical size of ions in solids and the ionic radii of Bi^{3+} and La^{3+} were taken to be identical.

For all of the selected compounds, the coordination numbers for the Bi^{3+} site (CN) and for the M^{n+} site (CN′) are given in Table 1. The possible substitution sites for Bi^{3+} ions are indicated in bold. The energy position and the literature assignment of the excitation bands are compiled in Tables 2 and 3. A few of the hosts contain two types of d^0 metal cations (for instance, YVO_4). In this case, the cation having the highest $\chi_{\mathrm{CN}'}(M^{n+})$ value was privileged for the calculation of MMCT energies; it is correspondingly underlined in the chemical formula (i.e., $\mathbf{Y}\underline{\mathbf{V}}\mathbf{O}_4$). Compounds containing both d^0 and d^{10} metal cations (for instance, $LaGaO_3$) were treated independently. Again, the considered metal is underlined (i.e., $\mathbf{La}\underline{\mathbf{Ga}}\mathbf{O}_3$ or $\mathbf{La}\underline{\mathbf{Ga}}\mathbf{O}_3$). Then, a compound noted as $\mathbf{La}\underline{\mathbf{Ga}}\mathbf{O}_3$ means that the Bi^{3+} ions enter at a La^{3+} site and that the nearby metal cation to which MMCT is considered is La^{3+}. The notation $\mathbf{La}\underline{\mathbf{Ga}}\mathbf{O}_3$ means that the Bi^{3+} ions enter at a La^{3+} site and that the nearby metal cation to which MMCT is considered is Ga^{3+}. Another example: the compound $NaYTiO_4$ is noted either $\mathbf{Na}\underline{\mathbf{Y}}\mathbf{Ti}\mathbf{O}_4$ or $\mathbf{Na}\underline{\mathbf{Y}}\mathbf{Ti}\mathbf{O}_4$. For both, the metal cation to which MMCT is considered is Ti^{4+}, but the Bi^{3+} ion occupies the Na^+ site in the former and the Y^{3+} site in the latter.

A few host lattices require specific comments:

- In the sequioxides ($\mathbf{M}_2\mathbf{O}_3$, where M = Sc or Y), only the C_2 site was retained, because it has a 75% probability of being occupied by Bi^{3+} dopant.
- In the garnets ($\mathbf{Y}_3\mathbf{Ga}_5\mathbf{O}_{12}$ and $\mathbf{Gd}_3\mathbf{Ga}_5\mathbf{O}_{12}$), the Ga^{3+} ions occupy 6-coordinated (CN′ = 6) and 4-coordinated (CN′ = 4) sites. Both situations were considered. The compounds are noted as $\mathbf{Y}_3\mathbf{Ga}_5\mathbf{O}_{12}$ (Ga[6]) and $\mathbf{Y}_3\mathbf{Ga}_5\mathbf{O}_{12}$ (Ga[4]), respectively. This raises the three following possibilities: $\mathbf{Y}_3\underline{\mathbf{Ga}}_5\mathbf{O}_{12}$ (Ga[6]), $\mathbf{Y}_3\underline{\mathbf{Ga}}_5\mathbf{O}_{12}$ (Ga[4]), and $\underline{\mathbf{Y}}_3\mathbf{Ga}_5\mathbf{O}_{12}$.
- In the orthorhombic perovskites ($\mathbf{Ca}\mathrm{MO}_3$ (where M = Ti, Zr) and $\mathbf{Na}\mathrm{NbO}_3$), Ca^{2+} and Na^+ are located in strongly distorted 12-coordinated sites that are characterized by 8 short distances and 4 long distances to nearby oxygen atoms. For all, a coordination number of 8 (CN = 8) was retained.

dx.doi.org/10.1021/ic400382k | Inorg. Chem. 2013, 52, 6028–6038

Table 1. List of the Host Lattices Selected in This Work[a]

	Host Lattice						
CN	CN′ = 4	CN′ = 6	CN′ = 7	CN′ = 8	CN′ = 9	CN′ = 10	CN′ = 12
4	$BiMg_2VO_6$						
5	$BiCaVO_5$		$LiYSiO_4$				
6	$BiMgVO_5$ $Bi_4Ge_3O_{12}$ $Bi_2Ge_3O_9$ $Bi_2Ga_4O_9$ (Ga[4])	$LiNbO_3$ M_2O_3 (M = Sc, Y) $ScBO_3$ MP_3O_9 (M = Sc, Y) $NaScO_2$, $LiScO_2$ $LiYO_2$, $NaYO_2$ Bi_2WO_6 $Bi_2W_2O_9$ $Na_3YSi_3O_9$ $YAl_3B_4O_{12}$ $CaYBO_4$ $InBO_3$, $GaBO_3$ $Bi_2Ga_4O_9$ (Ga[6])					
7	$Bi_{12}GeO_{20}$ $Bi_{12}TiO_{20}$	Bi_2MoO_6 $NaYTiO_4$ $Bi_{12}TiO_{20}$	La_2O_3, $LiYSiO_4$ $LaCdB_5O_{10}$ $LaZnB_5O_{10}$		$LaCdB_5O_{10}$		
8	$Bi_2Mo_2O_9$, $Bi_2(MoO_4)_3$ (l = 4) MVO_4 (M = Sc, Y, Gd) $CaMoO_4$, $CaWO_4$ Y_2WO_6, $Y_3Ga_5O_{12}$(Ga[4]), $Gd_3Ga_5O_{12}$ (Ga[4]) $SrGdGaO_5$	$CaMO_3$ (M = Ti, Zr) $NaYTiO_4$ $La_2Zr_2O_7$ YMO_4 (M = Nb, Ta) $GdNbO_4$, $LaNbO_4$ $GdTa_7O_{19}$ $Y_3Ga_5O_{12}$(Ga[6]) $Gd_3Ga_5O_{12}$ (Ga[6]) $LaGaO_3$ $LaInO_3$ $Y_2Sn_2O_7$ $Bi_2(MoO_4)_3$ (l = 6)		$Y_3M_5O_{12}$ (M = Al, Ga) MPO_4 (M = Sc, Y, La) LaP_3O_9, $Y_2Sn_2O_7$ $LaGaO_3$, $LaInO_3$ YBO_3 $La_2Zr_2O_7$			
9	$LaVO_4$		$LaCdB_5O_{10}$		$LaBO_3$ $LaCdB_5O_{10}$		
10						$LaZnB_5O_{10}$	
12							$LaAlO_3$

[a]CN = coordination number at the Bi^{3+} site (the substitution site is indicated in bold); CN′ = coordination number for the d^0 or the d^{10} metal (the considered metal is underlined when necessary).

The structure of YBO_3 has long been described on the basis of two very different Y^{3+} sites, with coordination numbers of 6 and 6 + 6.[23] According to Chadeyron et al.,[24] it appears that there is only one crystallographic position for the Y^{3+} ion in YBO_3 with a coordination number of 8; however, because of the random distribution of some oxygen atoms in the unit cell, two nonequivalent environments (with S_6 and C_3 symmetry) exist for Y^{3+} ions. The resulting distortion, however, remains small and does not affect the shortest Y−Y distance significantly.

The molybdates Bi_2MoO_6, $Bi_2MO_2O_9$, and $Bi_2(MoO_4)_3$ relate to the general family Bi_2O_3−$nMoO_3$, with n = 1 (γ-phase), n = 2 (β-phase), and n = 3 (α-phase). Their crystal structure is rather complex. It can be described on the basis of [MoO_l] and [BiO_m] polyhedra with several, but not necessarily all, oxygen shared. It is usually assumed that l = 6 for Bi_2MoO_6 (orthorhombic koechlinite form) and l = 4 for $Bi_2Mo_2O_9$. $Bi_2(MoO_4)_3$ is sometimes viewed as a distorted scheelite with ordered Bi^{3+} vacancies. In contrast to the other members, the Mo^{6+} ions have various oxygen coordinations that are so distorted that it is hard to decide whether l = 4, 5, or 6.[25,26] For this reason, the compound appears twice in Table 1, as $Bi_2(MoO_4)_3$ (l = 4) and $Bi_2(MoO_4)_3$ (l = 6), respectively. The situation with l = 5 was not considered.

3. RESULTS AND DISCUSSION

Many of the host lattices listed in Tables 2 and 3 were previously identified as MMCT-emitting compounds when doped with Bi^{3+}.[1,16,28,31,44−46,59] The luminescence behavior

dx.doi.org/10.1021/ic400382k | Inorg. Chem. 2013, 52, 6028−6038

Table 2. Structural and Spectroscopic Properties of Some Oxide Compounds Activated with Bi^{3+}: Electronic Configurations of $3d^0$, $4d^0$, and $5d^0$

M^{n+}	host lattice	$\chi_{CN'}(M^{n+})$	d_{corr} (Å)	excitation energy[a] (cm^{-1})	ref(s)
			Electronic Configuration of M^{n+} = $3d^0$		
Sc^{3+}	$\mathbf{Sc}_2O_3$	1.41	3.41	28600 (s), 30170 (A)+, 37470	27
				28700 (A)+	28
	$\mathbf{Sc}BO_3$	1.41	3.89	35100 (A)#	1
				35300 (A)#	23
	$\mathbf{Sc}P_3O_9$	1.41	5.57	39500 (A)#	29
	$\mathbf{Na}ScO_2$	1.41	3.28	27700 (A)+, 38700 (A)#	30
Ti^{4+}	$\mathbf{Ca}TiO_3$	1.73	3.19	27000 (CT)	16
	$Bi_{12}TiO_{20}$	2.02	3.71	27020, 27420	4
V^{5+}	$\mathbf{Sc}VO_4$	2.46	3	27780 (CT)	28
	$\mathbf{Y}VO_4$	2.46	3.21	29400 (CT)	1
				29670 (CT)	28
	$\mathbf{Gd}VO_4$	2.46	3.22	29600 (CT)	31
				30260 (A)−	32
				30500 (CT)	28
	$\mathbf{La}VO_4$	2.46	3.33	30860 (CT)	16
				30400 (A)−	32
	$BiCaVO_5$	2.46	3.51	30300 (CT)#	33
	$BiMgVO_5$	2.46	3.33	29150 (h)	34
	$BiMg_2VO_6$	2.46	3.74	22200	35
			Electronic Configuration of M^{n+} = $4d^0$		
Y^{3+}	$\mathbf{Y}_2O_3$	1.34	3.6	30100 (A)+, 38000	1
				28400 (s), 30960 (A)+, 38710	27
				28950 (A)+	28
				29400 (A)+	36
	$Li\mathbf{Y}O_2$	1.34	3.49	30800 (A)+	30
	$\mathbf{Li}YO_2$		3.22	30800 (A)+	
	$Na\mathbf{Y}O_2$	1.34	3.32	28300 (A)+, 39400 (A)?	30
	$\mathbf{Na}YO_2$		3.08	28300 (A)+, 39400 (A)+	
	$Na_3\mathbf{Y}Si_3O_9$	1.34	5.28	34360 (A)+	37
	$\mathbf{Na}_3YSi_3O_9$		3.3	34360 (A)?	
	$\mathbf{Y}Al_3B_4O_{12}$	1.34	5.94	36700 (A)+	38
	$Ca\mathbf{Y}BO_4$	1.34	3.49	35800 (A)?	38
	$\mathbf{Ca}YBO_4$		3.44	35800 (A)?	
	$Li\mathbf{Y}SiO_4$	1.31	3.72	35700 (A)+	38
	$\mathbf{Li}YSiO_4$		3.18	35700 (A)?	
	$\mathbf{Y}_3Al_5O_{12}$	1.29	3.74	36500 (A)+	15
				34800 (pairs)+, 37900 (A)+, 42340 (TE = CT) #	39
	$\mathbf{Y}_3Ga_5O_{12}$	1.29	3.82	32800 (CT)+, 38460 (h)+	40
				35200 (A, pairs)?	15
	$\mathbf{Y}BO_3$	1.29	3.84	38500 (A)?	1
				39200 (A)?	23
				37700 (A)?, 40500 (A)?	41
	$\mathbf{Y}PO_4$	1.29	3.83	43000 (A)#	1
	$\mathbf{Y}P_3O_9$	1.34	5.71	41500(A)+	29
	$\mathbf{Y}_2Sn_2O_7$	1.29	3.73	35700 (A)+, 34860 (pairs)+, 30770 (pairs)+	42
Zr^{4+}	$\mathbf{Ca}ZrO_3$	1.61	3.3	31250 (A)−	43
				32000 (A)−	15
	$\mathbf{La}_2Zr_2O_7$	1.61	4.68	34840 (A)+, 40820 (TE = CT)	44
Nb^{5+}	$\mathbf{Ca}Nb_2O_6$	1.86	3.47	31300 (CT)	16
	$\mathbf{Y}NbO_4$	1.86	3.61	31850 (CT)	45
				32300 (CT)	1
				32700 (CT)	46
				30800 (CT)	16
	$\mathbf{Gd}NbO_4$	1.86	3.62	32600 (A)?	47
				33000 (CT)	46

dx.doi.org/10.1021/ic400382k | Inorg. Chem. 2013, 52, 6028−6038

Table 2. continued

M^{n+}	host lattice	$\chi_{CN'}(M^{n+})$	d_{corr} (Å)	excitation energy[a] (cm^{-1})	ref(s)
			Electronic Configuration of M^{n+} = $4d^0$		
				31000 (CT)	16
	LaNbO_4	1.86	3.68	32800 (CT)	46
				31700 (CT)	16
Mo^{6+}	**Ca**MoO_4	2.5	3.69	30900 (CT)	16
				30300#	48
	Bi_2MoO_6	2.1	3.81	24390 (CT)?	49
	$Bi_2Mo_2O_9$	2.5	3.79	27400 (CT)?	
	$Bi_2(MoO_4)_3$ (l = 4)	2.5	3.53	27030 (CT)?	
	$Bi_2(MoO_4)_3$ (l = 6)	2.1	3.53	27030 (CT)	
			Electronic Configuration of M^{n+} = $5d^0$		
La^{3+}	**La**$_2O_3$	1.3	3.98	32470 (A)+, 40160	28
				32500 (A)+	38
				29400 (pairs)+, 32790 (A)+	36
	LaAlO_3	1.22	3.79	35090 (A)+	43
	LaBO_3	1.26	4.02	40400 (A)?	1
				36535 (pairs)?, 37260 (A)+	23
	LaPO_4	1.26	4.09	41500 (A)?	12, 38
				40800 (Bi^{3+}/PO_4^{3-} center)?	50
				39360 (A)?	51
	LaP_3O_9	1.28	4.31	42500 (A) ?	29
	LaZnB_5O_{10}	1.25	4.01	33560 (A)+	52
	LaCdB_5O_{10}	1.26	4.09	33900 (A)+	52
	LaCdB_5O_{10}		3.66		
	LaGaO_3	1.28	3.87	32470 (A)+	53
				32570 (A)+, 41670 (A)?	54
	LaInO_3	1.28	3.99	29400 (A)+	43
	La$_2Zr_2O_7$	1.28	4.68	34840 (A)+, 40820 (TE = CT)	44
Ta^{5+}	**Y**TaO_4	1.92	3.55	34500 (A)+	55
	GdTa_7O_{19}	1.92	3.74	32260 (CT)	16
				32260 (A)−	56
W^{6+}	**Ca**WO_4	2.59	3.73	36700 (A)+, 34800 (A)?	57
				33440, 39060 (A)+, 40800 (A)+	58
				35490 (WO_4^{2-}/Bi^{3+} center)+	59
	Y$_2$WO_6	2.59	3.34	29300 (CT)+	1, 60
	Bi_2WO_6	2.17	3.83	25640 (CT)?	49
	$Bi_2W_2O_9$	2.17	3.83	27030 (CT)+	49

[a]Legend: (A), literature assignment to A transition; (CT), literature assignment to the MMCT or TE transition; (s), shoulder; (h), host; (d) defects; +, confirmed literature assignment; ?, questionable literature assignment; −, erroneous literature assignment; and #, limit of the MMCT model. The underlined excitation energies obey eq 5 and, in this work, are assigned to the MMCT transition.

follows the situation depicted in Figure 1a. For these compounds, the CT excitation energies in Tables 2 and 3 are not underlined. An equation similar to eq 1 was then tentatively defined using these energies and the new set of data, i.e., d_{corr} and $\chi_{CN'}(M^{n+})$ with M = Ti, Zr, V, Nb, Ta, Mo and W. In contrast to the results reported in ref 16, it has not been possible to set up only one equation to account for the MMCT energies in these lattices. The compounds in which the M^{n+} cations are 4-coordinated are found to behave in a specific way (see Figure 2). This could be due to the more-covalent nature of the bond in tetra-coordinated systems, compared to larger coordination numbers. Two empirical equations are then provided, after least-squares refinement of the experimental data:

$$\mathrm{MMCT}(Bi^{3+}, cm^{-1}) = 70\,000 - 52\,000\frac{\chi_4(M^{n+})}{d_{corr}} \quad (3)$$

which is valid for 4-coordinated M^{n+} metals, and

$$\mathrm{MMCT}(Bi^{3+}, cm^{-1}) = 55\,000 - 45\,500\frac{\chi_{CN'>4}(M^{n+})}{d_{corr}} \quad (4)$$

which is valid for coordination numbers larger than 4. These equations allow prediction of the MMCT energies within an accuracy of ±3000 cm^{-1}. This value results from errors on the position of excitation bands (estimated at ±1500 cm^{-1}, depending on the experimental conditions (temperature, overlapping signals, spectral correction in the UV region, etc.); see Tables 2 and 3) and errors on the Bi^{3+}−M^{n+} distances (discrepancies on the values reported for d_{host} in the

dx.doi.org/10.1021/ic400382k | Inorg. Chem. 2013, 52, 6028−6038

Table 3. Structural and Spectroscopic Properties of Some Oxide Compounds Activated with Bi^{3+}: Electronic Configurations of $3d^{10}$ and $4d^{10}$

M^{n+}	host lattice	$\chi_{CN'}(M^{n+})$	d_{corr} (Å)	excitation energy[a] (cm^{-1})	ref(s)
		Electronic Configuration of M^{n+} = $3d^{10}$			
Zn^{2+}	**La**ZnB_5O_{10}	1.26[b]	3.63	33560 (A)+	52
Cd^{2+}	**La**CdB_5O_{10}	1.23[b]	3.66	33900 (A)+	52
	La**Cd**B_5O_{10}	1.23[b]	3.34		
Ga^{3+}	**La**GaO_3	1.58	3.29	32470 (A)+	53
				32570 (A)+, 41670(A)?	54
	GaBO_3	1.58	3.72[c]	36210 (A)+	61
				35800 (TE = CT)+	
	$Y_3Ga_5O_{12}$ (Ga[6])	1.58	3.5	32800 (CT)?, 38460 (h)?	40
				35200 (A, pairs)?	15
	$Y_3Ga_5O_{12}$ (Ga[4])	1.75	3.13	32800 (CT)+, 38460 (h)+	40
				35200 (A, pairs)+	15
	$Gd_3Ga_5O_{12}$ (Ga[6])	1.58	3.52	32260 (A)+, 37040 (h)+	40
	$Gd_3Ga_5O_{12}$ (Ga[4])	1.75	3.17	32260 (A)+, 37040 (h)?	40
	Sr**Gd**GaO_5	1.75	3.28	32000 (A)?	15
	SrGdGaO_5	1.75	3.24	32000 (A)?	
	$Bi_2Ga_4O_9$ (Ga[4])	1.75	3.54	26610, 37100	4
	$Bi_2Ga_4O_9$ (Ga[6])	1.58	3.31	26610, 37100	4
Ge^{4+}	$Bi_4Ge_3O_{12}$	2.11	3.59	37040 (CT)+	62, 13
				38460 (CT)+	63
	$Bi_2Ge_3O_9$	2.11	3.57	31050(A)+, 39520 (h)?	64
	$Bi_{12}GeO_{20}$	2.11	3.69	27420 (h)+, 28230 (d)	4
		Electronic Configuration of M^{n+} = $4d^{10}$			
In^{3+}	**La**InO_3	1.48	3.35	29400 (A)+	43
	InBO_3	1.48	3.89	35700 (CT − Bi^{3+}/In^{3+} TE)+	65
Sn^{4+}	$Y_2Sn_2O_7$	1.71	3.73	35700 (A)+, 34860 (pairs)?	42

[a]Legend: (A), literature assignment to A transition; (CT), literature assignment to the MMCT or TE transition; (s), shoulder; (h), host; (d) defects; +, confirmed literature assignment; ?, questionable literature assignment; −, erroneous literature assignment; and #, limit of the MMCT model. The underlined excitation energies obey eq 5 and, in this work, are assigned to the MMCT transition. [b]Values not tabulated in ref 19 and calculated as $\chi_7(Zn^{2+}) = {}^1/_2[\chi_6(Zn^{2+}) + \chi_8(Zn^{2+})] = 1.26$ and $\chi_7(Cd^{2+}) = {}^1/_2[\chi_6(Cd^{2+}) + \chi_8(Cd^{2+})] = 1.23$. [c]Estimated from the isostructural calcite structure of $InBO_3$ using the unit cell parameters given in ref 61.

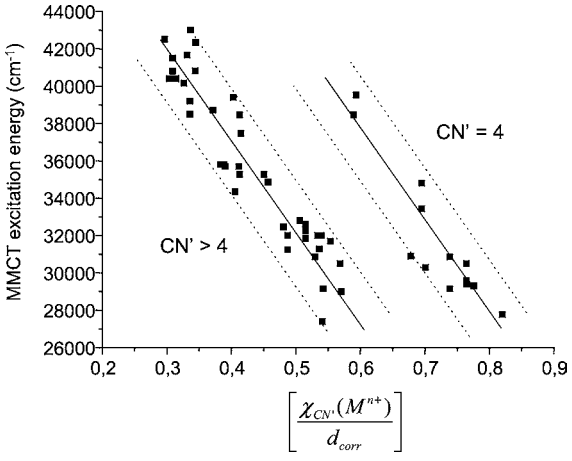

Figure 2. Variation of the $Bi^{3+} \rightarrow M^{n+}$ MMCT energy against the ratio $\chi_{CN'}(M^{n+})/d_{corr}$. Solid lines correspond to eqs 3 and 4; dotted lines indicate the limits of the model.

crystallographic databases and possible off-centered location of the Bi^{3+} ion, relative to the center of its coordination polyhedron, because of the stereochemical activity of the $6s^2$ lone pair). In the present work, an uncertainty of ±0.2 Å on the value of d_{corr} was considered. It induces an average error of ±0.05 on the ratio $\chi_{CN'}(M^{n+})/d_{corr}$. No error was considered on the $\chi_{CN'}(M^{n+})$ values. The above equations were then applied to all the other compounds listed in Tables 2 and 3. Only the excitation energies located within ±3000 cm^{-1} were retained. They are underlined in Tables 2 and 3. Figure 2 gives a global view of the situation.

Definition of a General Equation. Following the original approach of Jørgensen for charge-transfer energies and making the appropriate corrections in order to account for the structural differences among the host lattices, it is possible to express the empirical eqs 3 and 4 as a unique one that includes a difference of two terms: one related to the electron donor (Bi^{3+}) and one related to the electron acceptor (M^{n+}). The equation takes the general form

$$\mathrm{MMCT}(Bi^{3+}, cm^{-1}) = k_{CN'}\left[\chi_{CN}(Bi^{3+}) - \alpha^{CN}_{CN'}\frac{\chi_{CN'}(M^{n+})}{d_{corr}}\right] \quad (5)$$

where $k_{CN'}$ is a constant that is dependent on CN′, $\chi_{CN}(Bi^{3+})$ the electronegativity (EN) of Bi^{3+}, and $\alpha^{CN}_{CN'}$ an adjustable parameter that is dependent on CN and CN′. $\chi_{CN}(Bi^{3+})$ can be calculated for any value of CN, following the procedure given in Li and Xue:[19]

dx.doi.org/10.1021/ic400382k | Inorg. Chem. 2013, 52, 6028−6038

$$\chi_{CN}(Bi^{3+}) = \frac{0.105n^*}{r(Bi^{3+})}\sqrt{\frac{I_m}{13.6}} + 0.863 \quad (6)$$

where n^* is the effective principal quantum number (4.36), and I_m is the ultimate ionization energy (25.56 eV). The $k_{CN'}$ values were calculated as $70\,000/\chi_{CN}(Bi^{3+})$ for CN′ = 4 and $55\,000/\chi_{CN}(Bi^{3+})$ for CN′ > 4. The $\alpha^{CN}_{CN'}$ values were then obtained as $52\,000/k_4$ for CN′ = 4 and as $45\,500/k_{CN'}$ for CN′ > 4. The results are compiled in Tables 4 and 5. For a very rough estimation of MMCT energies, eq 5 can be operated using the average values $\overline{\chi}_{CN}(Bi^{3+}) = 1.35$, $\overline{k}_4 \approx 52000$ cm^{-1} (for 4-coordinated d^0 or d^{10} metals), or $\overline{k}_{CN'>4} \approx 41000$ cm^{-1} (for other coordination numbers) and $\overline{\alpha}^{CN}_{CN'} = 1$.

Table 4. Crystal Radii of Bi^{3+}, $\chi_{CN}(Bi^{3+})$, and $k_{CN'}$ Values

CN	$r(Bi^{3+})$ (Å)	$\chi_{CN}(Bi^{3+})$	k_4 (cm^{-1})	$k_{CN'>4}$ (cm^{-1})
5	1.10	1.43	48950	38461
6	1.17	1.40	50000	39285
7	1.24	1.37	51095	40145
8	1.31	1.34	52239	41044
9	1.35	1.33	52631	41353
10	1.41	1.305	53640	42145
12	1.50	1.28	54690	42970
		$\overline{\chi}_{CN}(Bi^{3+}) \approx 1.35$	$\overline{k}_4 \approx 52000$	$\overline{k}_{CN'>4} \approx 41000$

Table 5. $\alpha^{CN}_{CN'}$ Values

	$\alpha^{CN}_{CN'}$	
CN	CN′ = 4	CN′ = 6, 7, 8, 9
5	1.06	1.18
6	1.04	1.16
7	1.02	1.13
8	0.99	1.11
9	0.99	1.10
10	0.97	1.08
12	0.95	1.06
	$\overline{\alpha}^{CN}_{CN'} \approx 1$	$\overline{\alpha}^{CN}_{CN'} = 1.11$

Revisiting the Spectroscopy of Bi^{3+} Ions in Oxide Compounds. On the basis of the above results, it is interesting to revisit the literature assignment of the excitation bands in Bi^{3+}-doped oxide compounds. Let us start with the literature assignments that are not in contradiction with the model. For these, it is confirmed that the excitation bands ascribed to A transitions cannot be predicted by eq 5, within ±3000 cm^{-1}. Therefore, these data are considered to be correct and are labeled "+" in Tables 2 and 3. Note that a few signals that were not previously ascribed are now assigned to MMCT, since they obey eq 5. This, for instance, is the case for the high lying excitation signals in the Bi^{3+}-doped sesquioxides (i.e., 37 470 cm^{-1} in Sc_2O_3, 38 710 cm^{-1} in Y_2O_3, and 40 160 cm^{-1} in La_2O_3). For these, the spectroscopic behavior is consistent with Figure 1c. It is interesting to emphasize that the existence of a $Bi^{3+} \rightarrow Y^{3+}$ CT state was anticipated in the work by Van de Craats and Blasse[66] and is responsible for the quenching of the emission in Y_2O_3:Bi^{3+}. There are also a few cases for which a given excitation energy has been ascribed to either an A or CT (or TE) transition (i.e., $InBO_3$, $GaBO_3$, $LaVO_4$, $CaZrO_3$, $GdTa_7O_{19}$). For all these, the MMCT model holds.

More questionable are the excitation energies that were ascribed to an A transition but that are predicted by eq 5 (or vice versa, transitions assigned to CT but out of the model). These are indicated by the label "?" in Tables 2 and 3. This mark, however, does not mean that the literature assignment is systematically incorrect: an energy level structure similar to Figure 1b or the presence of bismuth pairs leads typically to ambiguous assignment. If we consider Figure 1b, two distinct emissions can be expected from the ^3P and MMCT states, respectively, since both states are excited by almost the same energy. In a more-accurate approach, the luminescence properties of Bi^{3+}-doped oxide compounds will now be discussed based on the 1-coordinate configuration diagrams sketched in Figure 3 (i.e. taking into account the lattice relaxation in the excited state). In contrast to Figure 1, this representation gives some qualitative information about Stokes shifts. Considering the nature of the excited states involved, the offset Δq is expected to be more pronounced for the MMCT state than for the intra-ionic $^3P_{1,0}$ state (i.e., $\Delta q' > \Delta q$). In the case depicted in Figure 3b, this will lead to a MMCT emission at longer wavelength and with a larger Stokes shift, compared to the localized $^3P_{1,0} \rightarrow {}^1S_0$ emission.[67]

Let us review a few results on these grounds: pyrochlores, phosphates, silicates, borates, gallates, lanthanum-based perovskites, stoichiometric compounds, and the relationship between the Stokes shift and trap depth.

Pyrochlores. *$LaZr_2O_7$:Bi^{3+}.* $LaZr_2O_7$:Bi^{3+} glows in the UV (385 nm) and in the yellow (515 nm) regions upon excitation

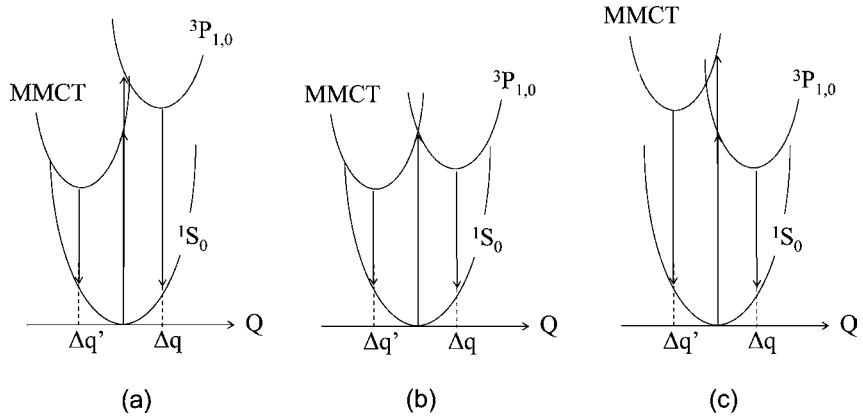

Figure 3. Schematic 1-coordinate energy level diagrams for Bi^{3+} ions in solids containing d^0 or d^{10} cations.

dx.doi.org/10.1021/ic400382k | Inorg. Chem. 2013, 52, 6028−6038

at 287 nm (34 800 cm^{-1}). The yellow emission is strongly favored after excitation at 245 nm (40 820 cm^{-1}). This latter energy is well-predicted by eq 5. It is assigned to $Bi^{3+} \rightarrow Zr^{4+}$ MMCT, in good agreement with the work of Srivastava and Beers.[44] The 287 nm band is also confirmed to be of the A type. This situation corresponds schematically to Figure 3c. The thermalization from ^3P to the MMCT state is invoked to account for the observed optical behaviors.[44]

$Y_2Sn_2O_7$:Bi^{3+}. $Y_2Sn_2O_7$:Bi^{3+} shows also two emissions, in the UV (330 nm) and in the yellow (515 nm) regions. The visible emission is excited at slightly lower energy (34 860 cm^{-1}) than the UV emission (35 700 cm^{-1}), but its Stokes shift is still larger. In contrast to $LaZr_2O_7$:Bi^{3+}, the relative intensity of the visible emission increases as the Bi^{3+} content is raised. This motivated the assignment of this emission to the formation of pairs.[42] It is known that Bi ions have a tendency to form clusters in glasses or in crystals. Many different types are reported, and some of them show near-infrared (NIR) luminescence.[68] Pairs can be perceived as molecular dimers, i.e., $(Bi^q)_2$ (where q represents the charge) or as two Bi ions located in nearby cationic sites. In the latter case, they may form a cluster with specific optical properties if the Bi−Bi distance is short enough to allow some orbital overlap. This is presumably the situation in $Y_2Sn_2O_7$:Bi^{3+}. In this compound, the $Bi^{3+} \rightarrow Y^{3+}$ MMCT would be in the vicinity of 40 000 cm^{-1} and will not be considered further. In contrast, the $Bi^{3+} \rightarrow Sn^{4+}$ MMCT is predicted at ∼35 000 cm^{-1} and is consistent with the observed excitation bands. This suggests a possible contribution of the MMCT process to the luminescence properties. Let consider that the 34 860 cm^{-1} band contains a MMCT contribution, superimposed with that of pairs. The corresponding situation would then be similar to that depicted in Figure 3b. In this frame, the same photon would induce either the MMCT, the A transition, or the Bi pairs emission if the dopant content is high enough. In the diluted compound (0.1 mol %), all the Bi^{3+} ions can be considered to be isolated. They are surrounded by six Y^{3+} cations and six Sn^{4+} cations at equal distance (3.73 Å; see Tables 2 and 3). In this situation, the emission spectrum shows a prominent UV band.[42] This indicates that (i) the A transition is much more probable than the MMCT transition in this compound and (ii) the contribution of this latter transition remains very limited.

Phosphates. *YPO_4:Bi^{3+}*. After the work of Jüstel et al.,[69] the emission of YPO_4:Bi^{3+} is composed of two bands, peaking at 245 and 335 nm, upon unique excitation at ∼230 nm (∼43000 cm^{-1}). The 245 nm emission is ascribed to $^3P_1 \rightarrow {}^1S_0$. The origin of the 335 nm band is not addressed. The excitation band at 43 000 cm^{-1} was ascribed to the A transition. It is worth noting that this excitation energy is also located at the limit of the model (see Tables 2 and 3). This suggests possible attribution of this band to $Bi^{3+} \rightarrow Y^{3+}$ MMCT as well. The situation would then be similar to Figure 3b. In this frame, the 335 nm emission could possibly be ascribed to the MMCT transition.

$LaPO_4$:Bi^{3+}. The case of $LaPO_4$:Bi^{3+} has been discussed in refs 12 and 50 and conducted to opposite conclusions. This compound is characterized by a blue emission at 450 nm upon excitation at 245 nm. The Stokes shift is very large. Moncorgé et al.[50] ascribed this band to a Bi^{3+}/PO_4^{3-} center, while Blasse et al.[12] ascribed it to an A transition. The present model does not support any of these assignments but suggests an attribution to $Bi^{3+} \rightarrow La^{3+}$ MMCT. The situation would then be similar to Figure 3a.

Silicates. $Na_3YSi_3O_9$ and $LiYSiO_4$ show a single emission at ∼350 nm when doped with Bi^{3+}. This emission was ascribed to an A transition. This assignment is confirmed only if Y^{3+} is the doping site in the compounds, which is, in fact, the most probable situation.

Borates. *$LaMB_5O_{10}$:Bi^{3+} (M = Zn, Cd) and $CaYBO_4$:Bi^{3+}*. The transitions in $LaMB_5O_{10}$:Bi^{3+} (M = Zn, Cd) are confirmed to be of the A type. Neither the $Bi^{3+} \rightarrow Zn^{2+}$ transition nor the $Bi^{3+} \rightarrow Cd^{2+}$ MMCT transition is demonstrated. In contrast, the position of the excitation band in $CaYBO_4$:Bi^{3+} is consistent with the MMCT transition, regardless of the considered doping site for the Bi^{3+} ions (Ca^{2+} or Y^{3+}).

MBO_3:Bi (M = In, Sc, Y, La). The TE (or MMCT) nature of the Bi^{3+} luminescence in $InBO_3$ is confirmed in the context of this work. This phosphor can be described using Figure 3a. The literature assignments in MBO_3:Bi (M = Sc, Y, La) are, in contrast, questionable. Let us briefly review the situation:

- $ScBO_3$:Bi shows a single excitation (35 000 cm^{-1}) and emission (33 400 cm^{-1}) ascribed to an A transition. For this compound, the predicted $Bi^{3+} \rightarrow Sc^{3+}$ MMCT is 3500 cm^{-1} larger than the experimental data. Considering the small Stokes shift and the presence of vibronic structures at low temperature that are not compatible with MMCT transitions, it comes out that the initial assignment can be considered as correct.
- YBO_3:Bi^{3+} shows two emission bands at 33 870 (34 000 cm^{-1} after the work of Chen et al.[41]) and 30 000 cm^{-1} (30 300 cm^{-1} after Chen et al.[41]), corresponding to two excitation bands at 39 210 cm^{-1} (40 485 cm^{-1} after Chen et al.[41]) and 37 900 cm^{-1} (37 730 cm^{-1} after Chen et al.[41]), respectively. The excitation signals were ascribed to A transitions. Taking the data reported in the work of Wolfert et al.,[23] these emission signals have different Stokes shifts (5340 and 7900 cm^{-1}) and were ascribed to Bi^{3+} ions located in two sites with coordination numbers of 6 and 6 + 6, the latter of which having the larger Stokes shift, because of the more-pronounced lattice relaxation. As mentioned in section 2, "Methodology", the Y^{3+} sites are 8-coordinated in YBO_3. This was confirmed in the work of Lin et al.[70] This makes the above assignment problematic. In this connection, the data reported in the work of Chen et al.[41] appear to be in better agreement with the structural features, considering that the Stokes shifts of the two emissions now differ by less than 1000 cm^{-1}. It is worth noting that the observed excitation signals in YBO_3:Bi^{3+} are also consistent with $Bi^{3+} \rightarrow Y^{3+}$ MMCT transitions. Nevertheless, taking into account a Stokes shift difference of <1000 cm^{-1} between the two emission signals, it seems unrealistic to ascribe one transition to MMCT and the other one to being A type. In addition, since the shortest Bi^{3+}−Y^{3+} distance is the same for both Y^{3+} sites, it is not possible to ascribe the two emissions to MMCT transitions. It is therefore concluded that the emission bands in YBO_3:Bi^{3+} are likely of A-type character, in agreement with the literature data.
- $LaBO_3$:Bi^{3+} also shows two emissions (27 900 and 21 700 cm^{-1}), corresponding to two strongly overlapping excitations, at 37 260 and 36 535 cm^{-1}. As there is only one possible site for the Bi^{3+} ions in this lattice, the emission with the larger Stokes shift was ascribed to Bi^{3+} pairs.[23] The Bi clusters in the $LaBO_3$ lattice is supposed

dx.doi.org/10.1021/ic400382k | Inorg. Chem. 2013, 52, 6028−6038

to result from an asymmetrical coordination of the Bi^{3+} ion within the La^{3+} site. Off-centered coordination is well-known for cations containing a lone pair (Tl^{+}, Pb^{2+}, Bi^{3+}, Sb^{3+}, etc.; see, for instance, the work of Galy and Meunier[71]) and has been confirmed to occur via EXAFS in $LaPO_4:Bi^{3+}$.[72] In this phosphate, it was found that the introduction of Bi^{3+} induces displacement of the nearby oxygen atoms toward positions occurring in $BiPO_4$. In stoichiometric compounds, it is considered that the stereochemical activity of the lone pair is approximately that of an anion such as O^{2-} or F^{-}. This reveals a high polarizability. A direct consequence, dealing with the Bi site, is a shortening of some $Bi^{3+}-O^{2-}$ bonds and a lengthening of some others. Taking the above example, the shortest La−O distance in $LaPO_4$ is 2.46 Å, while the shortest Bi−O distance in $BiPO_4$ is 2.33 Å.[73] This local distortion of the bismuth coordination polyhedron will certainly impact the second coordination sphere in such a way that the shortest $Bi^{3+}-La^{3+}$ distance in $LaPO_4:Bi^{3+}$ will be smaller than the shortest $La^{3+}-La^{3+}$ distance in undoped $LaPO_4$. Let us apply the same approach for the case of $LaBO_3:Bi^{3+}$. The shortest La−O distance in the borate is 2.45 Å, while the shortest distance in $BiBO_3$ is 2.15 Å.[74] It is interesting to note that a shortening of the same amount (0.3 Å) for the shortest $Bi^{3+}-La^{3+}$ distance in $LaBO_3:Bi^{3+}$ would lead to a $Bi^{3+} \rightarrow La^{3+}$ MMCT of ∼39 500 cm^{-1}, i.e., within ±3000 cm^{-1}, which is consistent with the experimental data. Within this frame, the corresponding scheme would be similar to Figure 3b, indicating that the 36 535 cm^{-1} excitation (for which the emission has a larger Stokes shift) could possibly contain a contribution of $Bi^{3+} \rightarrow La^{3+}$ MMCT while the other band would be of A type.

Gallates. *$M_3Ga_5O_{12}:Bi^{3+}$ (M = Y, Gd).* The luminescence behavior of $M_3Ga_5O_{12}:Bi^{3+}$ (M = Y, Gd) was investigated in 1994[40] and then revisited in 2006.[15] The compounds show emission in the UV region (31 250 cm^{-1}) and in the blue region (20 830 cm^{-1}). The corresponding excitations are given in Tables 2 and 3. There are a few discrepancies between the reports: in the work of Ilmer et al.,[40] it is shown that the host fundamental bands contribute to the blue emission; no UV emission was found. The luminescence processes in $(Y,Gd)_3Ga_5O_{12}:Bi^{3+}$ were ascribed to $Bi^{3+} \rightarrow Ga^{3+}$ MMCT. In the work of Setlur and Srivastava,[15] the UV emission was ascribed to A transition and the blue emission was attributed to Bi^{3+} pairs, considering that the blue emission intensity increases as the Bi^{3+} content in the material increases. In the compound $(Y_{0.75}Gd_{0.25})_3Ga_5O_{12}$, the corresponding excitations are located at 35 500 and 34 770 cm^{-1}, respectively. The clear presence of a shoulder at ∼33 500 cm^{-1} is also noted; however, no host sensitization is noticed.

Let us analyze this conflicting situation in light of the MMCT model. In these garnets, MMCT is possible between Bi^{3+} and Ga^{3+} ions located in 4- and 6-fold coordination. In $Y_3Ga_5O_{12}:Bi^{3+}$, an additional one (the $Bi^{3+} \rightarrow Y^{3+}$ MMCT) can also take place, but its value calculated using eq 5 (viz. 39 600 cm^{-1}) is larger than the bandgap. It will not be considered further. The other calculations give 29 900 cm^{-1} for $Bi^{3+} \rightarrow Ga^{3+}$ (CN′ = 4) and 34 600 cm^{-1} for $Bi^{3+} \rightarrow Ga^{3+}$ (CN′ = 6). Similar values are obtained for $Gd_3Ga_5O_{12}:Bi^{3+}$. This analysis reveals that the lowest lying excitation bands in the $(Y,Gd)_3Ga_5O_{12}:Bi^{3+}$ system could possibly be ascribed to $Bi^{3+} \rightarrow Ga^{3+}$ (CN′ = 6) MMCT, thus giving credit to the assignment made by Ilmer et al.[40] The luminescence characteristics of Bi^{3+} in these gallate garnets could then be interpreted on the basis of Figure 3b. Taking $(Y_{0.75}Gd_{0.25})_3Ga_5O_{12}:Bi^{3+}$ as an example, the 35 500 cm^{-1} band would be ascribed to an A transition and the 34 770 cm^{-1} band (or the underlying 33 500 cm^{-1} band) would be ascribed to $Bi^{3+} \rightarrow Ga^{3+}$ MMCT. It is important to note that the above analysis does not exclude the concomitant formation of bismuth pairs in the garnets. Looking at the excitation spectra, there is a striking similarity between $Y_{0.75}Gd_{0.25})_3Ga_5O_{12}:Bi^{3+}$ and $Y_2Sn_2O_7:Bi^{3+}$ and it reasonable to think that the arguments presented for the stannate holds for the gallate garnet as well.

The Perovskites $LaAlO_3$, $LaGaO_3$ and $LaInO_3$. The comparative investigation carried out by Srivastava on the Bi^{3+}-doped perovskites $LaAlO_3$, $LaGaO_3$, and $LaInO_3$, following the work of Van Steensel et al.,[43] is also very interesting. In the first compound, the only possible MMCT would occur between Bi^{3+} and La^{3+}, while in the two latter compounds, $Bi^{3+} \rightarrow Ga^{3+}$ and $Bi^{3+} \rightarrow In^{3+}$ MMCT could also take place. The calculated $Bi^{3+} \rightarrow La^{3+}$ MMCT energies are 39 950 ($LaGaO_3$), 40 400 ($LaInO_3$), and 40 350 cm^{-1} ($LaAlO_3$), while the $Bi^{3+} \rightarrow Ga^{3+}$ and $Bi^{3+} \rightarrow In^{3+}$ MMCT energies are calculated at 33 150 and 34 900 cm^{-1}, respectively. In all these compounds, the excitation signals were assigned to an A transition (see Tables 2 and 3). For $LaAlO_3:Bi^{3+}$ (35 100 cm^{-1}) and $LaInO_3:Bi^{3+}$ (29 400 cm^{-1}), these signals are indeed not consistent with MMCT transitions. Two excitation maxima are reported for $LaGaO_3:Bi^{3+}$ (∼32 500 and ∼41 700 cm^{-1}). The absorption edge for this host is located at ∼37 000 cm^{-1} (4.6 eV). This is in good correspondence with the high-energy part of the excitation spectrum reported by Srivastava[53] and suggests possible host sensitization of the bismuth emission. Careful inspection of this spectrum further indicates that the lowest lying band is not unique but consists of at least two largely overlapping components. One component can be ascribed to an A transition and the other one to $Bi^{3+} \rightarrow Ga^{3+}$ MMCT (predicted at 33 150 $cm^{-1} \approx 300$ nm). This would correspond to the situation depicted in Figure 3b.

Stoichiometric Compounds. Interesting luminescence properties are reported in bismuth-rich compounds containing germanate, vanadate, molybdate or tungstate complex groups (see Tables 2 and 3). In these compounds, the lowest conduction band states consist of M^{n+} (M = Ge^{4+}, V^{5+}, Mo^{6+}, W^{6+}) and Bi^{3+} 6p orbitals, while the top of the valence band is composed mostly of O^{2-} (2p) and Bi^{3+} (6s) orbitals. The optical properties result from electronic transitions between these orbitals. The formation of Frenkel, self-trapped, and multiple excitons is also mentioned.[62,75] It seems a general trend that the incorporation of bismuth in a metal oxide induces a narrowing of the host bandgap, because of additional hybridization of the occupied Bi^{3+} 6s and O^{2-} 2p orbitals that pushes up the top of the valence band.[76] This creates the possibility of observing $Bi^{3+} \rightarrow M^{n+}$ MMCT transitions at relatively low energy. Unfortunately, the MMCT model failed in predicting the energy of the lowest-lying excitation bands in most of the Bi^{3+}-rich compounds. This suggests that $Bi^{3+} \rightarrow M^{n+}$ MMCT (if any) is at higher energy than Bi^{3+} (6s) → Bi^{3+} (6p) transition or, in other words, that the M^{n+} orbitals are located higher than the Bi^{3+} 6p orbitals in the conduction band.

Because of the report by Timmermans and Blasse,[4] the luminescence of $Bi_{12}GeO_{20}$ (and of $Bi_{12}TiO_{20}$) is of the "semiconductor-type", i.e., the excitation into the band gap

dx.doi.org/10.1021/ic400382k | Inorg. Chem. 2013, 52, 6028−6038

yields free charge carriers, giving rise to photoconductivity. Following this idea, it is worth noting that several of the bismuth-rich compounds listed in Table 6 exhibit photo-

Table 6. Some Structural and Spectroscopic Characteristics of Bi^{3+}-Rich Compounds

compound	d_{corr} (Å)	shortest Bi^{3+}–Bi^{3+} distance (Å)	Exc (cm^{-1}) observed	MMCT (cm^{-1}) calculated
$Bi_2Mo_2O_9$	3.79	3.55	27400	35700
$BiMgV_2O_6$	3.74	3.53	22200	35800
Bi_2WO_6	3.83	3.69	25640	29200
$Bi_2W_2O_9$	3.83	3.69	27030	29200
Bi_2MoO_6	3.81	3.74	24390	29900
$BiCaVO_5$	3.51	3.47	30300	33550
$Bi_{12}GeO_{20}$	3.69	3.71	27420, 28230	40265
$Bi_{12}TiO_{20}$	3.71	3.61	27020, 27420	41700
$BiMgVO_5$	3.33	3.40	29150	31600
$Bi_2(MoO_4)_3$ (l = 4)	3.53	3.73	27030	33170
$Bi_2(MoO_4)_3$ (l = 6)	3.53	3.73	27030	27930
$Bi_4Ge_3O_{12}$	3.59	3.88	34500, 37040	39440
$Bi_2Ge_3O_9$	3.57	4.08	31050, 39520	39265
$Bi_2Ga_4O_9$ (Ga[4])	3.31	4.17	26610, 37100	44300
$Bi_2Ga_4O_9$ (Ga[6])	3.54	4.17	26610, 37100	33280

catalytic properties, including $Bi_{12}TiO_{20}$, Bi_2MoO_6, $Bi_2MO_2O_9$, Bi_2WO_6, and $BiMg_2VO_6$.[74−80] This property involves the generation and migration of photogenerated charge carriers upon band-gap excitation, thus confirming a semiconductor character. It is interesting to note the presence of relatively short Bi^{3+}–Bi^{3+} distances in these compounds, i.e., shorter or in the same range than the shortest Bi^{3+}–M^{n+} distances (Table 6). This could favor the formation of bismuth-related Frenkel excitons.

The optical transitions of $Bi_2Ge_3O_9$, $Bi_4Ge_3O_{12}$, and $Bi_2Ga_4O_9$ are considered, in the work of Timmermans and Blasse,[4] to be more localized and it is worth noting that the Bi^{3+}–Bi^{3+} distances in these compounds are significantly longer than the shortest Bi^{3+}–M^{n+} distances. The same holds for $BiMgVO_5$ and $Bi_2(MoO_4)_3$. From Table 6, we note, for a few compounds, that there is a coincidence (within ±3000 cm^{-1}) between the observed (underlined) and calculated MMCT excitation energies. This could possibly represent a contribution of the MMCT process. However, some problematic issues remain: $Bi_2Ga_4O_9$ is not predicted (regardless of the coordination of the Ga^{3+} ions); $Bi_2W_2O_9$ is predicted, although the Bi^{3+}–Bi^{3+} distance is shorter than the shortest Bi^{3+}–M^{n+} distance in the compound; and $Bi_2(MoO_4)_3$ is predicted only if we describe the network with MoO_6 octahedra (i.e., l = 6). This analysis leads us to conclude that the application of the MMCT model is still uncertain for stoichiometric compounds and that additional data are required to give more credit to this interpretation.

On the Relationship between the Stokes Shift and the Small $^3P_1$–$^3P_0$ Trap Depth. As mentioned in the Introduction section, there is some controversy about the origin of very small trap depth (i.e., < 25 cm^{-1}) and its connection with large Stokes shift values in Bi^{3+}-activated compounds. This question will be now discussed at the light of the MMCT model. The case of bismuth-rich compounds will not be addressed here as the MMCT model is not confirmed as applicable. However, it is noticed that the trap depth in the stoichiometric compounds seems to be very small (<25 cm^{-1}; see ref 4). The known values of trap depths, Stokes shifts, and emission character of some compounds investigated in this paper are compiled in Table 7.

Table 7. Trap Depths, Stokes Shifts, and Emission Character of Some Bi^{3+}-Doped Oxide Compounds

host lattice	CN	trap depth (cm^{-1})	ref	Stokes shift (cm^{-1})	emission character
Y_2O_3	6	113	27	5100	A
$ScBO_3$	6	968	23	1600	A
$NaScO_2$	6	610	30	1530	A
La_2O_3	7	371	12	9360	A
$LaPO_4$	8	16	12	19300	MMCT
YVO_4	8	8	81	12120	MMCT
$LaGaO_3$	8	500	53	6000	A
$LaBO_3$	9	443	23	9360	A
		46		14835	pairs or MMCT

From these data, the connection between large Stokes shifts and small trap depth seems to be confirmed. The agreement is less obvious with the coordination number of the site occupied by Bi^{3+} ions. In contrast, there seems to be a relationship between the small trap depths and the MMCT process. Unfortunately, the available data are too scarce to confirm this trend unambiguously. The knowledge of trap depths values in $InBO_3$:Bi^{3+} and $LaVO_4$:Bi^{3+} would, for instance, be of great interest in this connection.

4. CONCLUSION

The concept of charge transfer between Bi^{3+} and d^0 or d^{10} cations, although not new, is first formalized in the present paper for any coordination of the considered cations. The model is shown to provide new insights on the interpretation of the spectroscopic behavior of Bi^{3+} ions in oxide compounds through the rationalization of the spectral assignments. As far as the crystal structure of the host lattice is known, the model can be extended to any type of d^0 or d^{10} cations, in any coordination and to non-oxidic compounds. However, its applicability still must be confirmed for stoichiometric compounds. It is hoped that this new, user-friendly tool could be helpful for the design of efficient phosphors incorporating Bi^{3+} ions as emitters or as sensitizers for rare-earths or transition metals.

AUTHOR INFORMATION

Corresponding Author

*Tel.: +33(0)4 73407100. E-mail address: Philippe.Boutinaud@ensccf.fr.

Notes

The authors declare no competing financial interest.

REFERENCES

(1) Blasse, G.; Bril, A. *J. Chem. Phys.* **1968**, *48*, 217−222.
(2) Blasse, G. *J. Lumin.* **1997**, *72*−*74*, 129−134.
(3) Wang, L.; Sun, Q.; Liu, Q.; Shi, J. *J. Solid State Chem.* **2012**, *191*, 142−146.
(4) Timmermans, C. W. M.; Blasse, G. *J. Solid State Chem.* **1984**, *52*, 222−232.

(5) Real, F.; Vallet, V.; Flament, J. P.; Schamps, J. *J. Chem. Phys.* **2006**, *125*, 174709.
(6) Real, F.; Vallet, V.; Flament, J. P.; Schamps, J. *J. Chem. Phys.* **2007**, *127*, 104705.
(7) Real, F.; Ordejon, B.; Vallet, V.; Flament, J. P.; Schamps, J. *J. Chem. Phys.* **2009**, *131*, 194501.
(8) Boulon, G.; Jorgensen, C. K.; Reisfeld, R. *Chem. Phys. Lett.* **1980**, *75*, 24−26.
(9) Boulon, G.; Pedrini, C.; Guidoni, M.; Pannel, C. *J. Phys. (Paris)* **1975**, *36*, 267−278.
(10) Boulon, G.; Moine, B.; Bourcet, J. C.; Reisfeld, R.; Kalisky, Y. *J. Lumin.* **1979**, *18−19*, 924−928.
(11) Boulon, G.; Faurie, J. P.; Madej, C. *J. Solid State Chem.* **1974**, *10*, 167−174.
(12) Blasse, G.; Van der Steen, A. C. *Solid State Commun.* **1979**, *31*, 993−994.
(13) Moncorgé, R.; Jacquier, B.; Boulon, G. *J. Lumin.* **1976**, *14*, 337−348.
(14) Blasse, G. *Struct. Bonding (Berlin)* **1991**, *76*, 153−187.
(15) Setlur, A. A.; Srivastava, A. M. *Opt. Mater.* **2006**, *29*, 410−415.
(16) Boutinaud, P.; Cavalli, E. *Chem. Phys. Lett.* **2011**, *503*, 239−243.
(17) Jørgensen, C. K. *Prog. Inorg. Chem.* **1970**, *12*, 101−158.
(18) Bergerhoff, G.; Brown, I. D. *Crystallographic Databases—Information Content, Software Systems, Scientific Applications*; Allen, F. H., Bergerhoff, G., Sievers, R., Eds.; Data Commission of the International Union of Crystallography: Bonn, Germany, 1987.
(19) Li, K.; Xue, D. *J. Phys. Chem. A* **2006**, *110*, 11332−11337.
(20) Li, K.; Xue, D. *Phys. Status Solidi B* **2007**, *244*, 1982−1987.
(21) Krumpel, A. H.; Boutinaud, P.; Van der Kolk, E.; Dorenbos, P. *J. Lumin.* **2010**, *130*, 1357−1365.
(22) Shannon, R. D. *Acta Crystallogr., Sect. A: Cryst. Phys., Diffr., Theor. Gen. Crystallogr.* **1976**, *32*, 751−767.
(23) Wolfert, A.; Oomen, E. W. J. L.; Blasse, G. *J. Solid State Chem.* **1985**, *59*, 280−290.
(24) Chadeyron, G.; El Ghozzi, M.; Mahiou, R.; Arbus, A.; Cousseins, J. C. *J. Solid State Chem.* **1997**, *128*, 261−266.
(25) Li, Y.; Chen, G.; Zhang, H.; Li, Z.; Sun, J. *J. Solid State Chem.* **2008**, *181*, 2653−2659.
(26) Mestl, G.; Linsmeir, C.; Gottschall, R.; Dieterle, M.; Find, J.; Herein, D.; Jäger, J.; Uchida, Y.; Schlögl, R. *J. Mol. Catal. A: Chem.* **2000**, *162*, 463−492.
(27) Bordun, O. M. *J. Appl. Spectrosc.* **2002**, *69*, 67−71.
(28) Boulon, G. *J. Phys. (Paris)* **1971**, *32*, 333−347.
(29) Oomen, E. W. J. L.; Blasse, G. *J. Solid State Chem.* **1988**, *75*, 201−204.
(30) Van der Steen, A. C.; Van Hesteren, J. J. A.; Slok, A. P. *J. Electrochem. Soc.* **1981**, *128*, 1327−1333.
(31) Mahalley, B. N.; Dhoble, S. J.; Pode, R. B.; Alexander, G. *Appl. Phys. A: Mater. Sci. Process.* **2000**, *70*, 39−45.
(32) Park, W. J.; Jung, M. K.; Jung, S. J.; Yoon, D. H. *Colloids Surf. A* **2008**, *313−314*, 373−377.
(33) Pei, Z.; Van Dijken, A.; Vink, A.; Blasse, G. *J. Alloys Compd.* **1994**, *204*, 243−246.
(34) Benmokthar, S.; El Jazouli, A.; Chaminade, J. P.; Gravereau, P.; Guillen, F.; de Waal, D. *J. Solid State Chem.* **2004**, *177*, 4175−4182.
(35) Huang, J.; Sleigth, A. W. *J. Solid State Chem.* **1992**, *100*, 170−178.
(36) Van de Craats, A. M.; Blasse, G. *Chem. Phys. Lett.* **1995**, *243*, 559−563.
(37) Kim, C. H.; Park, H. L.; Mho, S. *Solid State Commun.* **1997**, *101*, 109−113.
(38) Blasse, G. *J. Solid State Chem.* **1972**, *4*, 52−54.
(39) Zorenko, Y.; Gorbenko, V.; Voznyak, T.; Jary, V.; Nikl, M. *J. Lumin.* **2010**, *130*, 1963−1669.
(40) Ilmer, M.; Grabmaier, B. C.; Blasse, G. *Chem. Mater.* **1994**, *6*, 204−206.
(41) Chen, L.; Zheng, H.; Cheng, J.; Song, P.; Yang, G.; Zhang, G.; Wu, C. *J. Lumin.* **2008**, *128*, 2027−2030.
(42) Srivastava, A. M. *Mater. Res. Bull.* **2002**, *37*, 745−751.
(43) Van Steensel, L. I.; Bokhov, S. G.; Van de Craats, A. M.; De Blank, J.; Blasse, G. *Mater. Res. Bull.* **1995**, *30*, 1359−1362.
(44) Srivastava, A. M.; Beers, W. W. *J. Lumin.* **1999**, *81*, 293−300.
(45) Shin, S. H.; Jeon, D. Y.; Suh, K. S. *J. Appl. Phys.* **2001**, *90*, 5986−5990.
(46) Park, T. K.; Ahn, H. C.; Mho, S. *J. Korean Phys. Soc.* **2008**, *52*, 431−434.
(47) Liu, X. M.; Lin, J. *J. Lumin.* **2007**, *122−123*, 700−703.
(48) Xie, A.; Yuan, X.; Hai, S.; Wang, J.; Li, L. *J. Phys. D: Appl. Phys.* **2009**, *42*, 105107.
(49) Blasse, G.; Boon, L. *Ber. Bunsen. Phys. Chem.* **1984**, *88*, 929−930.
(50) Moncorgé, R.; Boulon, G.; Denis, J. *J. Phys. C* **1979**, *12*, 1165−1171.
(51) Wang, D.; Wang, Y. H. *Mater. Res. Bull.* **2007**, *42*, 2163−2169.
(52) Jagannathan, R.; Manoharan, S. P.; Rao, R. P.; Kutty, T. R. N. *Jpn. J. Appl. Phys.* **1991**, *29*, 1991−1996.
(53) Srivastava, A. M. *Mater. Res. Bull.* **1999**, *34*, 1391−1396.
(54) Jacquier, B.; Boulon, G.; Sallavuard, G.; Gaume-Mahn, F. *J. Solid State Chem.* **1972**, *4*, 374−378.
(55) Blasse, G.; Bril, A. *J. Lumin.* **1970**, *3*, 109−131.
(56) Kubota, S.-I.; Yamane, H.; Shimada, M. *J. Alloys Compd.* **1998**, *281*, 181−185.
(57) Zorenko, Y.; Pashkovsky, M.; Voloshinovskii, A.; Kuklinski, B.; Grinberg, M. *J. Lumin.* **2006**, *116*, 43−51.
(58) Pode, R. B.; Dhoble, S. J. *Phys. Status Solidi B* **1997**, *203*, 571−577.
(59) Nagirnyi, V.; Kotlov, A.; Jönsson, L.; Kirm, M.; Lushchik, A. *Nucl. Instrum. Methods Phys. Res., A* **2005**, *537*, 61−65.
(60) Tian, L.; Yang, P.; Wu, H.; Li, F. *J. Lumin.* **2010**, *130*, 717−721.
(61) Dotsenko, V. P.; Efryushina, N. P.; Berezovskaya, I. V. *Mater. Lett.* **1996**, *28*, 517−520.
(62) Moncorgé, R.; Jacquier, B.; Boulon, G.; Gaume-Mahn, F.; Janin, J. *J. Lumin.* **1976**, *12/13*, 467−472.
(63) Blasse, G.; Grabmaier, B. C. *Luminescent Materials*; Springer−Verlag: Berlin, Heidelberg, Germany, 1994.
(64) Timmermans, C. W. M.; Boen, Ho O.; Blasse, G. *Solid State Commun.* **1982**, *42*, 505−507.
(65) Blasse, G.; de Mello Donega, C.; Berezovskaya, I. V.; Dotsenko, V. *Solid State Commun.* **1994**, *91*, 29−31.
(66) Van de Craats, A. M.; Blasse, G. *Mater. Res. Bull.* **1996**, *31*, 381−387.
(67) de Blank, J.; Blasse, G. *Eur. J. Solid State Inorg. Chem.* **1996**, *33*, 295−307.
(68) Sokolov, V. O.; Plotnichenko, V. G.; Dianov, E. M. *Opt. Lett.* **2008**, *33*, 1488−1490.
(69) Jüstel, T.; Huppertz, P.; Mayr, W.; Wiechert, D. U. *J. Lumin.* **2004**, *106*, 225−233.
(70) Lin, J.; Sheptyakov, D.; Wang, Y.; Allenspach, P. *Chem. Mater.* **2004**, *16*, 2418−2424.
(71) Galy, J.; Meunier, G. *J. Solid State Chem.* **1975**, *13*, 142−159.
(72) Van Zon, F. B. M.; Koningberger, D. C.; Oomen, E. W. J. L.; Blasse, G. *J. Solid State Chem.* **1987**, *71*, 396−402.
(73) Romero, B.; Bruque, S.; Aranda, M. A. G.; Iglesias, J. E. *Inorg. Chem.* **1994**, *33*, 1869−1874.
(74) Becker, P.; Fröhlich, R. *Z. Naturforsch., B: Chem. Sci.* **2004**, *59*, 256−258.
(75) Itoh, M.; Katagiri, T. *J. Phys. Soc. Jpn.* **2010**, *79*, 074717.
(76) Li, Y.; Chen, G.; Zhang, H.; Li, Z.; Sun, J. *J. Solid State Chem.* **2008**, *181*, 2653−2659.
(77) Fu, H.; Pan, C.; Wao, W.; Zhu, Y. *J. Phys. Chem. B* **2005**, *109*, 22432−22439.
(78) Zhou, J.; Zou, Z.; Ray, A. K.; Zhao, X. S. *Ind. Eng. Chem. Res.* **2007**, *46*, 745−749.
(79) Li, H.; Li, K.; Wang, H. *Mater. Chem. Phys.* **2009**, *116*, 134−142.
(80) Guo, R.; Zhang, G.; Liu, J. *Mater. Res. Bull.* **2013**, *48*, 1857−1863.
(81) Moncorgé, R.; Boulon, G. *J. Lumin.* **1979**, *18/19*, 376−380.